Published in final edited form as:

Cell Rep. 2021 September 07; 36(10): 109670. doi:10.1016/j.celrep.2021.109670.

C. elegans LIN-28 controls temporal cell fate progression by regulating LIN-46 expression via the 5′ UTR of *lin-46* mRNA

Orkan Ilbay[1,2], **Charles Nelson**[1], **Victor Ambros**[1,3,*]

[1]Program in Molecular Medicine, University of Massachusetts Medical School, 373 Plantation Street, Worcester, MA 01605, USA

[2]Department of Pathology, Stanford University School of Medicine, Stanford, CA 94305, USA

[3]Lead contact

SUMMARY

Lin28/LIN-28 is a conserved RNA-binding protein that promotes proliferation and pluripotency and can be oncogenic in mammals. Mammalian Lin28 and *C. elegans* LIN-28 have been shown to inhibit biogenesis of the conserved cellular differentiation-promoting microRNA *let-7* by directly binding to unprocessed *let-7* transcripts. Lin28/LIN-28 also bind and regulate many mRNAs in diverse cell types. However, the determinants and consequences of LIN-28-mRNA interactions are not well understood. Here, we report that *C. elegans* LIN-28 represses the expression of LIN-46, a downstream protein in the heterochronic pathway. We find that *lin-28* and sequences within the *lin-46* 5′ UTR are required to prevent LIN-46 expression at early larval stages. Moreover, we find that precocious LIN-46 expression caused by mutations in the *lin-46* 5′ UTR is sufficient to cause precocious heterochronic defects similar to those of *lin-28(lf)* animals. Thus, our findings demonstrate the biological importance of the regulation of individual target mRNAs by LIN-28.

In brief

Ilbay et al. characterize the role of the 5′ UTR of *lin-46*, a heterochronic gene in *C. elegans* and the critical mRNA target of the widely conserved RNA-binding protein LIN-28, demonstrating the importance of the regulation of mRNAs by LIN-28 *in vivo* along with the conserved microRNA *let-7*.

Graphical Abstract

*Correspondence: victor.ambros@umassmed.edu.

AUTHOR CONTRIBUTIONS

Conceptualization, O.I. and V.A.; methodology, O.I. and V.A.; formal analysis, O.I. and V.A.; investigation, O.I. and C.N.; resources, V.A.; writing – original draft, O.I.; writing – review & editing, O.I., V.A., and C.N.; visualization, O.I.; funding acquisition, V.A.

DECLARATION OF INTERESTS

The authors declare no competing interests.

SUPPLEMENTAL INFORMATION

Supplemental information can be found online at https://doi.org/10.1016/j.celrep.2021.109670.

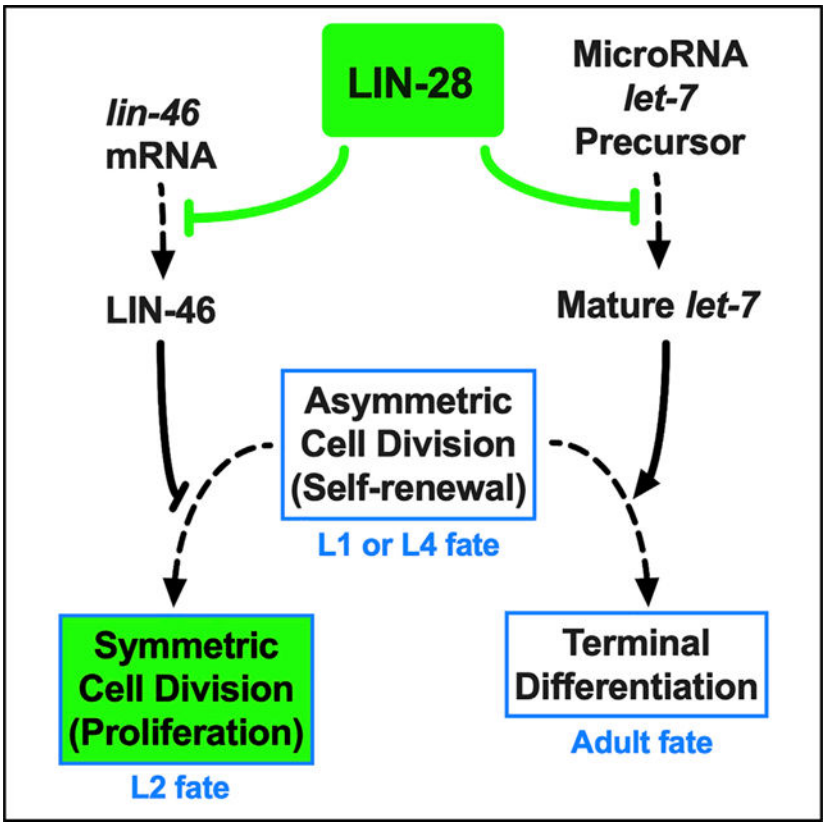

INTRODUCTION

Animal development involves complex cell lineages within which different cell fates are executed in specific orders and at a pace that is in synchrony with overall developmental rate. *C. elegans* develops through four larval stages (L1–L4), each of which involves an invariant set of cell division and cell fate specification events (Sulston and Horvitz, 1977). The precise timing of cell-fate transitions within individual cell lineages is regulated by genes in the heterochronic pathway (Ambros and Horvitz, 1984; Rougvie and Moss, 2013). In this pathway, three major temporal regulatory transcription factors control the transitions from earlier to later cell fates. These transcription factors are directly or indirectly regulated by microRNAs and/or RNA-binding proteins, thereby facilitating proper cell-fate transitions during larval development.

One of the transcription factors in the heterochronic pathway, Hunchback-like-1 (HBL-1), is expressed at the L1 and L2 stages and is downregulated during the L2-to-L3 transition (Abrahante et al., 2003; Ilbay and Ambros, 2019a). HBL-1 promotes L2-stage symmetric cell divisions and prevents progression to L3-stage asymmetric cell divisions (Abrahante et al., 2003; Lin et al., 2003). In *hbl-1 loss of function* (*lf*) mutant larvae, hypodermal stem cells skip L2-specific symmetric cell divisions and precociously transition to asymmetric cell divisions (that are normally characteristic of the L3 stage), resulting in reduced numbers of hypodermal cells, and premature terminal differentiation of the hypodermis. By contrast, mutations that cause ectopic HBL-1 activity at the L3 and L4 stages lead to

reiterations of L2 cell division patterns and hence extra hypodermal cells (Ilbay and Ambros, 2019b). During the L2-to-L3 transition, HBL-1 is regulated by *let-7*-family microRNAs (*mir-48/84/241*; Abbott et al., 2005) and by *lin-28* (Abbott et al., 2005; Vadla et al., 2012), which acts on *hbl-1* indirectly via a protein coding gene *lin-46* (Ilbay and Ambros, 2019b; Pepper et al., 2004).

LIN-28 is a conserved RNA-binding protein first identified as a heterochronic gene product in *C. elegans* (Ambros and Horvitz, 1984). Like HBL-1, LIN-28 is downregulated between the L2 and L3 stages (Moss et al., 1997). *lin-28(lf)* mutants exhibit precocious development in the hypodermis similar to *hbl-1(lf)*, including deletion of L2 cell fates, precocious vulva development, and premature terminal differentiation (Ambros and Horvitz, 1984). LIN-28 inhibits the maturation of the conserved microRNA *let-7* (Van Wynsberghe et al., 2011), which is required for this hypodermal differentiation at the end of the L4 stage (Reinhart et al., 2000). Curiously, although *let-7* is expressed precociously at the early stages in *lin-28(lf)* larvae and *let-7* function is required for the precocious terminal differentiation of hypodermal cells in *lin-28(lf)* animals, *let-7* is not required for the skipping of L2-stage proliferative cell fates observed in *lin-28(lf)* (Vadla et al., 2012). Instead, the effect of *lin-28* on the timing of the L2-to-L3 cell-fate transition is mediated by a protein coding gene, *lin-46*. *lin-46(lf)* mutations suppress *lin-28(lf)* precocious phenotypes (Pepper et al., 2004), indicating that disregulation of LIN-46 could be responsible for the precocious expression of L3 through adult cell fates in *lin-28(lf)* larvae (Vadla et al., 2012). Previous studies indicated that *C. elegans* LIN-28 binds to the *lin-46* mRNA *in vivo* (Stefani et al., 2015), but the consequence of this binding is not known.

Although LIN-46 exhibits evolutionary conservation of protein sequence (Feng et al., 1998; Fritschy et al., 2008), the molecular functions of LIN-46 have not been clear. However, our recent findings suggest that LIN-46 affects temporal cell fates in *C. elegans* by inhibiting the nuclear accumulation of HBL-1 (Ilbay and Ambros, 2019b). Therefore, it is possible that LIN-28 could promote L2 fates by inhibiting the premature expression of LIN-46 during the L2. Here, we show that LIN-46 is expressed only at the L3 and L4 stages in a temporal profile that is the inverse of LIN-28, which is expressed at the L1 and L2 stages. We find that LIN-46 is expressed precociously in *lin-28(lf)* animals, supporting the hypothesis that LIN-28 represses LIN-46 expression in the L1 and L2. We find that mutations in the 5′ UTR of *lin-46* result in precocious LIN-46 expression in the hypodermal stem cells and precocious cell lineage phenotypes similar to *lin-28(lf)*. Our results indicate that precocious LIN-46 expression can account for the majority of the *lin-28(lf)* phenotypes and support the critical importance of the LIN-28-LIN-46 axis in the temporal regulation of HBL-1 in *C. elegans*.

RESULTS

lin-28 represses LIN-46 expression during early larval stages

To characterize the expression dynamics of LIN-28 and LIN-46 in developing larvae, we used CRISPR-Cas9 to tag *lin-28* and *lin-46* with fluorescent proteins at their endogenous loci (Figure 1A). We found that the expression pattern of endogenously tagged LIN-28::GFP is similar to that reported previously for a transgene expressing tagged LIN-28 (Moss

et al., 1997): LIN-28 is highly expressed in embryos and in L1- and L2-stage larvae and is diminished at subsequent larval stages (Figures 1B and 1C). The expression pattern of endogenously tagged LIN-46::mCherry differs from the pattern previously reported for a *lin-46* transcriptional reporter transgene (Pepper et al., 2004): We observed LIN-46::mCherry predominately in hypodermal seam cells and in the ventral hypodermal vulval precursor cells (VPCs) at the L3 and L4 stages (Figures 1B and 1C; Table S1). Our finding that LIN-46::mCherry expression is restricted to the L3 and L4 stages, combined with a previous report indicating that *lin-46* transcription occurs at all larval stages (Pepper et al., 2004), suggests that *lin-46* is post-transcriptionally regulated.

The expression pattern of endogenously tagged LIN-28 and LIN-46 reveals that the developmental dynamics of LIN-28 and LIN-46 are mutually exclusive (Figure 1C), suggesting that LIN-28 may repress LIN-46 expression during the L1 and L2 larval stages. To test this supposition, we examined the effect of *lin-28(lf)* on the expression pattern of LIN-46::mCherry and found that LIN-46 is expressed precociously at the L1 and L2 stages in *lin-28(lf)* animals (Figures 1B and 1C), consistent with the conclusion that LIN-28 represses LIN-46 expression at these early larval stages.

Mutations in the *lin-46* 5′ UTR result in *lin-28(lf)*-like phenotypes and precocious LIN-46 expression

The finding that LIN-46 is expressed precociously at the L1 and L2 stages in *lin-28(lf)* animals indicates that LIN-28 could directly repress LIN-46 expression by binding to the *lin-46* mRNA, as suggested by a previous study showing that LIN-28 could crosslink to *lin-46* mRNA *in vivo* (Stefani et al., 2015), and as supported by previous genetic epistasis findings that *lin-46* functions downstream of *lin-28* (Pepper et al., 2004). However, although *lin-46* activity was shown to be necessary for the precocious phenotypes of *lin-28(lf)* (Pepper et al., 2004), LIN-28 appears to have hundreds of direct targets (Stefani et al., 2015), and it is not known whether LIN-46 expression alone could be sufficient for the precocious phenotypes of *lin-28(lf)* mutants.

We sought to test for the phenotypic consequences of LIN-46 expression uncoupled from repression by *lin-28* by mutating putative LIN-28-interacting sequences in the *lin-46* mRNA sequence. We noticed that the *lin-46* 5′ UTR exhibits unusually high sequence conservation among nematodes (Figure S1A) and contains a GGAG motif that is often associated with LIN-28/Lin28 binding (Stefani et al., 2015; Wilbert et al., 2012; Figures S1A and S1B). Therefore, we targeted the *lin-46* 5′ UTR using a CRISPR guide (Figures S1A and S1B) and observed frequent *lin-28(lf)*-like phenotypes in the F1/F2 progeny of the injected animals (Figure S1C). We found a range of *lin-46* 5′ UTR deletions varying in size (2–19 bp) in animals expressing *lin-28(lf)*-like phenotypes (Figure S1D).

To determine the effects of the *lin-46* 5′ UTR mutations on the expression of LIN-46, we injected the CRISPR mix containing the guide targeting the *lin-46* 5′ UTR into animals carrying the *lin-28::gfp [lin-28(ma426)]* and *lin-46::mCherry [lin-46(ma398)]* alleles (Figure 1A; Table S2) and found that *lin-46* 5′ UTR deletion mutations resulted in precocious LIN-46::mCherry expression at the L1 and L2 stages (Figures 1A–1C). This result shows that an intact *lin-46* 5′ UTR is required for proper LIN-46 expression. Importantly, our

CRISPR mutagenesis of the *lin-46* 5′ UTR did not affect the expression of LIN-28 (Figures 1B and 1C). Thus, LIN-46 is expressed precociously in *lin-46* 5′ UTR mutants despite the presence of LIN-28, suggesting that the *lin-46* 5′ UTR likely mediates LIN-28 binding to *lin-46* mRNA and consequent repression of LIN-46 protein. We interpret these *lin-46* 5′ UTR mutations to confer *lin-46 gain of function* (*gf*), in the sense that they alleviate the repression of LIN-46 expression by LIN-28. Thus, we will refer to the set of deletions in the 5′ UTR of *lin-46* described in this study (Figure S1D) as *lin-46(gf)* alleles.

Next, we determined whether the mutations in the *lin-46* 5′ UTR affected *lin-46* mRNA levels. We found that *lin-46* mRNA is expressed at the L1 and L2 stages in wild-type animals (Figure S2). In *lin-28(lf)* and *lin-46(gf)*, the *lin-46* mRNA is also expressed at the L1 and L2 stages at similar levels to wild type (Figure S2). Therefore, the precocious LIN-46 expression in *lin-28(lf)* and *lin-46(gf)* mutants is likely due to an increase in the translatability of the *lin-46* mRNA in these mutants rather than an increase in the *lin-46* mRNA level.

Precocious LIN-46 expression causes precocious cell-fate transitions in hypodermal seam cell lineages

To compare the heterochronic phenotypes of the *lin-46(gf)* mutants to those of a *lin-28(lf)* mutant, we assessed the number of seam cells, the timing of *col-19p*::*gfp* expression (a reporter for terminal differentiation of hypodermal cells), and the timing of the formation of an adult-specific cuticle structure called alae (Figure 2).

All three *lin-46(gf)* mutants tested had fewer seam cells than wild type (Figure 2A), reflective of skipping the L2-stage symmetric seam cell divisions, similar to *lin-28(lf)* mutants. The severity of this seam cell phenotype varies among the various *lin-46(gf)* mutants and is overall somewhat weaker than that of *lin-28(lf)* (Figure 2A). In doubly mutant animals containing *lin-46(gf)* alleles in combination with *lin-28(lf)* (Figure 2A), the presence of a *lin-46(gf)* allele did not enhance the seam cell number phenotype of *lin-28(lf)* (Figure 2A), indicating that the *lin-46* 5′ UTR and *lin-28* act in the same pathway.

Also similar to *lin-28(lf)*, seam cells in *lin-46(gf)* mutants precociously express adult fates during larval stages, as demonstrated by the precocious expression of *col-19p::gfp* (Figure 2B) and the precocious formation of adult alae in L4-stage larvae (Figure 2C).

In *lin-28(lf)* mutants, *let-7* microRNA is required for the precocious expression of adult cell fates (Vadla et al., 2012). Similarly, we found that *let-7* microRNA was required for the expression of adult cell fates in *lin-46(gf)* mutants: in *lin-46(ma461gf); let-7(n2853)* double mutants, precocious alae expression was not observed, and similarly, precocious *col-19p::gfp* expression was largely suppressed (Figure 2B). The residual precocious *col-19p::gfp* expression in some seam cells of *lin-46(ma461gf); let-7(n2853)* animals (Figure 2B) could reflect the fact that HBL-1, the target of LIN-46 (Ilbay and Ambros, 2019b), functions not only in the L2-to-L3 seam cell fate transition but also contributes to the larva-to-adult transition downstream of *let-7* (Vadla et al., 2012).

LIN-46 is expressed in the VPCs, and precocious LIN-46 expression leads to precocious onset of vulva development

During *C. elegans* larval development, stem cells of the ventral hypodermal lineages P3–P8 divide during the L1 stage and give rise to the six VPCs (Sulston and Horvitz, 1977). After their birth in the L1 stage, the VPCs temporarily arrest in the G1 phase of the cell cycle until the L3 stage, when they undergo a single round of cell division (Figure 3A; Euling and Ambros, 1996). Soon after this initial VPC cell division, three of the six VPCs (P5.p, P6.p, and P7.p) undergo additional rounds of cell divisions, giving rise to 22 cells that differentiate and form the adult vulva (Figure 3A).

The timing of the first VPC divisions in the mid-L3 stage is controlled by genes in the heterochronic pathway, including *lin-28* (Ambros and Horvitz, 1984; Euling and Ambros, 1996). In *lin-28(lf)* mutants, the first VPC divisions precociously take place in the L2 stage, followed by accelerated completion of vulva cell divisions by approximately the mid-L3 stage and precocious execution of vulva morphogenetic processes prior to the L3 molt, resulting in the appearance of a morphologically abnormal ("protruding") vulva (Pvl) on the ventral surface of L4 animals (Ambros and Horvitz, 1984; Euling and Ambros, 1996; Figure 3C). Loss of *lin-46* suppresses the Pvl phenotype caused by *lin-28(lf)* (Pepper et al., 2004). However, because LIN-46 expression in the VPCs had not been previously detected using transgenic reporters (Pepper et al., 2004), it was not clear how loss of *lin-46* could affect the precocious vulva phenotype of *lin-28(lf)* animals.

We found that endogenously tagged LIN-46 is expressed in the VPCs at the L3 and L4 stages (Figure 3A), which coincides with the developmental period when the VPCs produce the adult vulva (Figure 3A). In *lin-28(lf)* mutants (Figure 3B, left) or in *lin-46(gf)* mutants (Figure 3B, right), LIN-46 is precociously expressed in the L2-stage VPCs, coincident with the precocious onset of vulva development of these mutants. These results indicate that precocious LIN-46 expression is sufficient to accelerate the timing of VPC cell division and subsequent vulva cell divisions and morphogenesis (Figure 3C) and that precocious LIN-46 expression is likely to be responsible for the majority of the phenotypes observed in *lin-28(lf)* animals.

Altogether, our results are consistent with the model that LIN-46 suppresses L2 cell fates in lateral hypodermal seam cells and in VPCs and that LIN-28 restricts LIN-46 expression until after the L2, whereupon upregulation of LIN-46 promotes transitions to L3 cell fates for these cell lineages.

The predicted architecture of the *lin-46* 5′ UTR is conserved

Most *C. elegans* transcripts are *trans*-spliced, resulting in the presence of a 22-nt splice-leader (SL) RNA sequence at the 5′ end of the mRNA (Blumenthal, 2012). The presence of an up-stream splice acceptor "TTTCAG" (Figure S1B) and expressed sequence tag (EST) clones that contain the *SL1-lin-46*-5′ UTR fusion sequence (e.g., GenBank: FN875625.1) indicate that *lin-46* mRNA is *trans*-spliced.

We used the RNAfold Webserver (Gruber et al., 2008) to predict the structure of the *SL1-lin-46*-5′ UTR fusion sequence (Figure4A). The predicted structure of the *SL1-lin-46*-5′

UTR chimeric RNA shows base pairing between *SL1* and the first 8 nucleotides (nts) at the 5′ end of the *lin-46* 5′ UTR (Figure 4A; "*SL1*-complementary"). The 16 nts that follow the *SL1*-complementary region are conserved among all *Caenorhabditis* species analyzed in this study (with the exception of a single nucleotide in *C. inopinata*) and constitute a "single-stranded stretch" region (Figures 4A and 4B). The last 12 nts in the *lin-46* 5′ UTR contains a conserved GGAG sequence that is located in the stem of a predicted stem-loop structure (Figure 4A; "stem-loop"). The sequence conservation patterns in *SL1*-complementary and stem-loop regions (Figure 4B) are consistent with the biological relevance and significance of the predicted structures: nucleotide changes that preserve base pairing and mutations in the loop region (presumably not contributing to the hairpin stability) appear to be more tolerated.

The single-stranded stretch was the region primarily targeted by our CRISPR guide used to generate the 5′ UTR mutants (Figures S1B and S1D). Mutations of various sizes in this region (Figures S1D and 4B) displayed precocious LIN-46 expression (Figures 1A–1C; *ma459gf*) and strong *lin-28(lf)*-like phenotypes (Figure 2A; *ma461gf*). Interestingly, in certain *lin-46(gf)* mutants, such as *ma459* and *ma461*, that result in strong precocious phenotypes, the predicted RNA structure is entirely altered (Figure 4C), which may indicate a causative relationship between loss of structural elements in the *lin-46* 5′ UTR and a strong loss of LIN-46 repression.

Interestingly, although the GGAG motif was found to be enriched in LIN-28 bound RNA regions (Stefani et al., 2015) and is considered to be a putative LIN-28 motif (Wilbert et al., 2012), our findings suggest that presence of the GGAG sequence in the *lin-46* 5′ UTR is not alone sufficient to confer repression of LIN-46, because the *ma472* mutation leaves the GGAG motif intact (Figure 4C) yet causes strong *lin-46(gf)* phenotypes (Figures 2 and 3).

DISCUSSION

By examining the expression patterns of endogenously tagged *C. elegans* LIN-28 and its regulatory target LIN-46, and by employing genetic and phenotypic analysis, we show that LIN-28 and the 5′ UTR of *lin-46* prevent LIN-46 expression in early larval stages and that *lin-46* mis-regulation can account for the precocious developmental phenotypes observed in *lin-28(lf)* animals. Our results suggest that LIN-28 controls temporal cell fate progression by regulating LIN-46 expression via the 5′ UTR of *lin-46* mRNA (Figure 4D).

In addition to repressing LIN-46 expression, LIN-28 inhibits the maturation of *let-7* microRNA. Therefore, in *lin-28(lf)* mutants, both LIN-46 and mature *let-7* microRNA are precociously expressed, and the former promotes precocious cell fate progression at early larval stages whilst the latter promotes precocious expression of adult cell fates in the L4. Interestingly, *lin-46(lf)* fully suppresses the precocious adult cell fate defects in *lin-28(lf); lin-46(lf)* doubly mutant larvae, even though *let-7* microRNA still appears to be abundant in samples of total RNA from L2 larvae (Nelson and Ambros, 2019; Vadla et al., 2012). It is possible that this precocious accumulation of *let-7* microRNA in *lin-28(lf); lin-46(lf)* L2 larvae reflects non-hypodermal expression of *let-7* and that the normal timing of adult cell fates in *lin-28(lf); lin-46(lf)* reflects restoration of proper *let-7* developmental dynamics

in the hypodermis, perhaps via HBL-1-mediated repression of *let-7* expression (Roush and Slack, 2009).

The *C. elegans lin-28-lin-46* pathway acts in parallel to *let-7*-family microRNAs (Abbott et al., 2005; Vadla et al., 2012) and regulates the nuclear localization, and hence the activity, of the critical *let-7*-family target HBL-1 (Ilbay and Ambros, 2019b). Indeed, the LIN-46-mediated repression of HBL-1 nuclear localization is a potent substitute for microRNA repression of HBL-1 translation; for example, precocious LIN-46 expression conferred by the *lin-46(gf)* mutants can fully compensate for the deletion of all 10 *let-7*-complementary sites in the *hbl-1* 3′ UTR (Ilbay and Ambros, 2019b), which otherwise causes a severe retarded cell fate phenotype due to persistent HBL-1 activity (Ilbay and Ambros, 2019b).

Limitations of the study

We hypothesize that LIN-28 likely regulates LIN-46 production at the level of translation and that binding of LIN-28 to the *lin-46* 5′ UTR is required for LIN-28-mediated repression of LIN-46 expression. Evidence in support of this hypothesis include (1) previously reported high-throughput sequencing of RNA isolated by crosslinking immunoprecipitation (HITS-CLIP) data indicating that LIN-28 associates with *lin-46* mRNA *in vivo* (Stefani et al., 2015), (2) our analysis of *lin-46* mRNA levels in *lin-28* and *lin-46(gf)* mutants (Figure S2), and (3) the phenotypic similarities between *lin-28(lf)* and the *lin-46(gf)* mutants (Figures 1, 2, and 3).

We also hypothesize that the mutations in the *lin-46* 5′ UTR described here reduce LIN-28 binding, permitting the precocious translation of the *lin-46* mRNA. However, we did not directly test this hypothesis, and there are also several related questions that we were not able to address, including the following: (1) is the 5′ UTR of *lin-46* sufficient to confer *lin*-28-dependent repression of mRNA translation? (2) Does LIN-28 binding to the 5′ UTR of *lin-46* affect LIN-28 binding to other regions of the *lin-46* mRNA? (3) What are the contributions of LIN-28 binding in different regions of the *lin-46* mRNA to the regulation of translation? (4) Does LIN-28 bind the *lin-46* 5′ UTR *in vitro*, and would such *in vitro* assays reflect *in vivo* binding potential of LIN-28 to the 5′ UTR of *lin-46*?

With enough time and resources, most of these questions could be answered using experimental tools based on current technology—including *in vivo* reporter constructs containing the 5′ UTR of *lin-46*, HITS-CLIP, and electrophoretic mobility shift assay (EMSA) experiments to measure LIN-28 binding to wild-type and mutant 5′ UTR of *lin-46 in vivo* and *in vitro*—and would provide valuable insights into how LIN-28 interacts with and regulates its mRNA targets.

STAR★METHODS

RESOURCE AVAILABILITY

Lead contact—Further information and requests for reagents should be directed to and will be fulfilled by the Lead Contact, Victor Ambros, (victor.ambros@umassmed.edu).

Materials availability—All unique/stable reagents generated in this study are available from the Lead Contact with a completed materials transfer agreement.

Data and code availability

- Data reported in this paper will be shared by the Lead Contact upon request.
- This paper does not report original code.
- Any additional information required to reanalyze the data reported in this paper is available from the Lead Contact upon request.

EXPERIMENTAL MODEL AND SUBJECT DETAILS

C. elegans* culture conditions—C. elegans* strains used in this study and corresponding figures in the paper are listed in Table S2 and also in Key resources table. *C. elegans* strains were maintained at 20°C on nematode growth media (NGM) and fed with the *E. coli* HB101 strain (See Key resources table).

METHOD DETAILS

Assaying extra seam cell and Pvl phenotypes—The worms were scored at the young adult stage (determined by the gonad morphology) for the number of seam cells using fluorescence microscopy with the help of the *maIs105[col-19p::gfp]* transgene that marks the lateral hypodermal cell nuclei and/or for protruding vulva phenotype (Pvl) by examining the vulva morphology (as given in Figure 3C).

Microscopy—All DIC and fluorescent images are obtained using a ZEISS Imager Z1 equipped with ZEISS Axiocam 503 mono camera, and the ZEN Blue software (See Key resources table). Prior to imaging, worms were anesthetized with 0.2 mM levamisole in M9 buffer and mounted on 2% agarose pads. Fore each fluorescent reporter (*col-19p::gfp*, *lin-28::gfp,* or *lin-46::mCherry*), all images in a comparison set were captured using identical microscope, camera, and exposure settings and identical post-processing by ImageJ Fiji software (See Key resources table). For each condition, the expression pattern shown is representative of is observed in 100% of 10 animals observed (Figures 1B and 3).

Fluorescent tagging of lin-28 and lin-46 using CRISPR/Cas9—A mixture of plasmids encoding SpCas9 (pOI90, 70 ng/μL), and single guide RNAs (sgRNAs) targeting the site of interest (60 ng/μL of pSW65 for *lin-28* or pOI113 for *lin-46*) and the unc-22 gene (pOI91, 30 ng/μL) as co-CRISPR marker, a donor plasmid (20 ng/μL of pOI173 for lin-28 or pOI167 for *lin-46*) containing the gfp or mCherry sequence flanked by gene-specific homology arms, and a rol-6(su1006) containing plasmid (pOI124, 30 ng/μL) as co-injection marker, was injected into the germlines of ten young adult worms. F1 roller and/or twitcher animals (100–200 worms) were cloned and screened by PCR amplification (Table S3) for the presence of the expected homologous recombination (HR) product. F2 progeny of F1 clones positive for the HR-specific PCR amplification product were screened for homozygous HR edits by PCR amplification of the locus using primers that flanked the HR arms used in the donor plasmid (Table S3). Finally, the genomic locus spanning the HR arms and *gfp* or *mCherry* DNA was sequenced using Sanger sequencing. A single worm with a

precise HR edited *lin-28* or *lin-46* locus was cloned and backcrossed twice before used in the experiments.

CRISPR/Cas9-mutagenesis of the lin-46 5′UTR—A mixture of plasmids encoding SpCas9 (pOI90, 70 ng/μL), and gR_5U single guide RNA (sgRNAs) targeting the *lin-46* 5′UTR (Figure S2; pOI193 60 ng/μL) was injected into the germlines of young adult worms expressing the adult onset *gfp* transgene, *col-19p::gfp* (Table S2; VT1357). F1 or F2 animals displaying precocious cell fate phenotypes, which were consisted of precocious *col-19p::gfp* expression in the seam cells (Figure S1C) and protruding vulva morphology (Figure 3C), were cloned and genotyped for in-del events at the gR_5U targeting site (Figure S1D).

Quantitative PCR—Samples of total RNA were pre-treated with turbo DNase (Invitrogen). cDNA was synthesized using SuperScript IV (See Key resources table) following the manufacturer's instructions, using the RT oligonucleotides (Table S3). qPCR reactions were performed using CoWin Biosciences FastSYBR Mixture (Low Rox) (See Key resources table) following the manufacturer's instructions, using a Viia 7 Real Time PCR System (Applied Biosystems) (qPCR primers: Table S3). ΔCTs were calculated by normalizing samples to *gpd-1* (*GAPDH*). ΔCTs were then inverted so that greater values reflect greater RNA levels, and were normalized to set the value of the least abundant sample to one. For each biological replicate, the average of three technical replicates was used.

QUANTIFICATION AND STATISTICAL ANALYSIS

Each circle on the genotype versus number of seam cells plots shows the observed number of seam cells on one side of a single young adult worm. A minimum of 20 worms for each genotype were analyzed and the average number of seam cells (mean) was denoted by vertical bars in the genotype versus number of seam cell plots. Percent Pvl values were calculated (n = 20 young adult worms) and represented as a bar graph. The Student's t test was used to calculate statistical significance when comparing different genotypes. The GraphPad Prism 8 software (See Key resources table) was used to plot the graphs and for statistical analysis.

Supplementary Material

Refer to Web version on PubMed Central for supplementary material.

ACKNOWLEDGMENTS

We thank Sungwook Choi (Watts Lab, UMass Medical School, Worcester) for sharing the pSW65 plasmid expressing a CRISPR guide RNA, which we used to tag *lin-28* with GFP. We thank the laboratory of Martin Chalfie (Columbia University) for critical reading of the preprint. This research was supported by funding from NIH grants R01GM088365 and R01GM034028 (V.A.).

REFERENCES

Abbott AL, Alvarez-Saavedra E, Miska EA, Lau NC, Bartel DP, Horvitz HR, and Ambros V (2005). The let-7 microRNA family members mir-48, mir-84, and mir-241 function together to regulate developmental timing in Caenorhabditis elegans. Dev. Cell 9, 403–414. [PubMed: 16139228]

Abrahante JE, Daul AL, Li M, Volk ML, Tennessen JM, Miller EA, and Rougvie AE (2003). The Caenorhabditis elegans hunchback-like gene lin-57/hbl-1 controls developmental time and is regulated by microRNAs. Dev. Cell 4, 625–637. [PubMed: 12737799]

Ambros V, and Horvitz HR (1984). Heterochronic mutants of the nematode Caenorhabditis elegans. Science 226, 409–416. [PubMed: 6494891]

Blumenthal T (2012). Trans-splicing and operons in *C. elegans*. WormBook, 1–11.

Euling S, and Ambros V (1996). Heterochronic genes control cell cycle progress and developmental competence of C. elegans vulva precursor cells. Cell 84, 667–676. [PubMed: 8625405]

Feng G, Tintrup H, Kirsch J, Nichol MC, Kuhse J, Betz H, and Sanes JR (1998). Dual requirement for gephyrin in glycine receptor clustering and molybdoenzyme activity. Science 282, 1321–1324. [PubMed: 9812897]

Fritschy J-M, Harvey RJ, and Schwarz G (2008). Gephyrin: where do we stand, where do we go? Trends Neurosci. 31, 257–264. [PubMed: 18403029]

Gruber AR, Lorenz R, Bernhart SH, Neuböck R, and Hofacker IL (2008). The Vienna RNA websuite. Nucleic Acids Res. 36, W70–W74. [PubMed: 18424795]

Ilbay O, and Ambros V (2019a). Pheromones and nutritional signals regulate the developmental reliance on let-7 family microRNAs in C. elegans. Curr. Biol. 29, 1735–1745.e4. [PubMed: 31104929]

Ilbay O, and Ambros V (2019b). Regulation of nuclear-cytoplasmic partitioning by the *lin-28-lin-46* pathway reinforces microRNA repression of HBL-1 to confer robust cell-fate progression in *C. elegans*. Development 146, dev183111. [PubMed: 31597658]

Lin S-Y, Johnson SM, Abraham M, Vella MC, Pasquinelli A, Gamberi C, Gottlieb E, and Slack FJ (2003). The *C. elegans hunchback* homolog, *hbl-1*, controls temporal patterning and is a probable MicroRNA target. Dev. Cell 4, 639–650. [PubMed: 12737800]

Moss EG, Lee RC, and Ambros V (1997). The cold shock domain protein LIN-28 controls developmental timing in C. elegans and is regulated by the lin-4 RNA. Cell 88, 637–646. [PubMed: 9054503]

Nelson C, and Ambros V (2019). Trans-splicing of the *C. elegans let-7* primary transcript developmentally regulates *let-7* microRNA biogenesis and *let-7* family microRNA activity. Development 146, dev172031. [PubMed: 30770392]

Pepper AS-R, McCane JE, Kemper K, Yeung DA, Lee RC, Ambros V, and Moss EG (2004). The C. elegans heterochronic gene lin-46 affects developmental timing at two larval stages and encodes a relative of the scaf-folding protein gephyrin. Development 131, 2049–2059. [PubMed: 15073154]

Reinhart BJ, Slack FJ, Basson M, Pasquinelli AE, Bettinger JC, Rougvie AE, Horvitz HR, and Ruvkun G (2000). The 21-nucleotide let-7 RNA regulates developmental timing in Caenorhabditis elegans. Nature 403, 901–906. [PubMed: 10706289]

Rougvie AE, and Moss EG (2013). Developmental transitions in C. elegans larval stages. Curr. Top. Dev. Biol 105, 153–180. [PubMed: 23962842]

Roush SF, and Slack FJ (2009). Transcription of the C. elegans let-7 microRNA is temporally regulated by one of its targets, hbl-1. Dev. Biol. 334, 523–534. [PubMed: 19627983]

Stefani G, Chen X, Zhao H, and Slack FJ (2015). A novel mechanism of LIN-28 regulation of let-7 microRNA expression revealed by in vivo HITS-CLIP in C. elegans. RNA 21, 985–996. [PubMed: 25805859]

Sulston JE, and Horvitz HR (1977). Post-embryonic cell lineages of the nematode, Caenorhabditis elegans. Dev. Biol. 56, 110–156. [PubMed: 838129]

Vadla B, Kemper K, Alaimo J, Heine C, and Moss EG (2012). lin-28 controls the succession of cell fate choices via two distinct activities. PLoS Genet. 8, e1002588. [PubMed: 22457637]

Van Wynsberghe PM, Kai ZS, Massirer KB, Burton VH, Yeo GW, and Pasquinelli AE (2011). LIN-28 co-transcriptionally binds primary let-7 to regulate miRNA maturation in Caenorhabditis elegans. Nat. Struct. Mol. Biol 18, 302–308. [PubMed: 21297634]

Wilbert ML, Huelga SC, Kapeli K, Stark TJ, Liang TY, Chen SX, Yan BY, Nathanson JL, Hutt KR, Lovci MT, et al. (2012). LIN28 binds messenger RNAs at GGAGA motifs and regulates splicing factor abundance. Mol. Cell 48, 195–206. [PubMed: 22959275]

Highlights

- An intact 5′ UTR of *lin-46* is necessary to prevent precocious cell fate progression
- LIN-28 and 5′ UTR of *lin-46* prevent precocious LIN-46 expression
- LIN-46 is expressed in the vulval precursor cells and stimulates vulva development

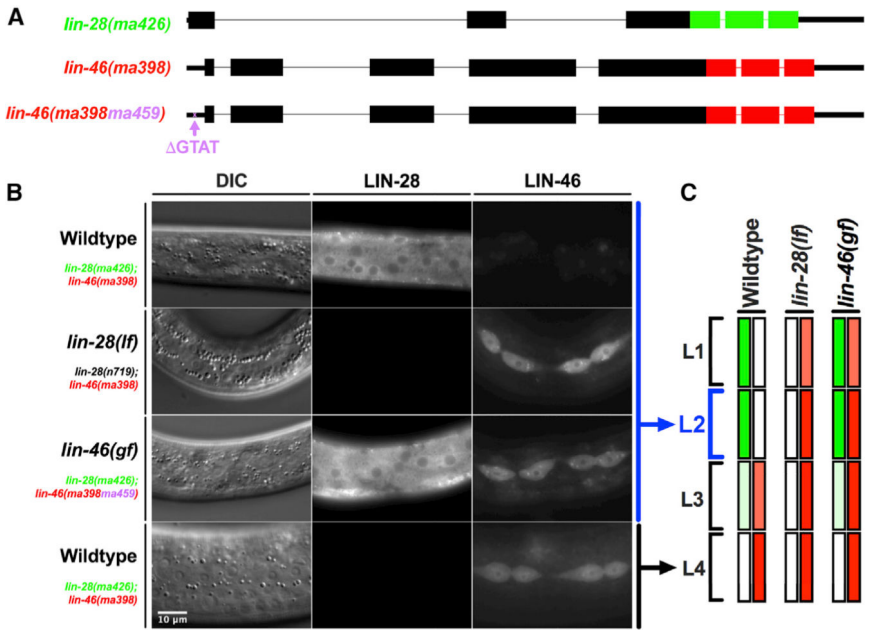

Figure 1. *lin-28* and *lin-46* 5′ UTR prevent LIN-46 expression at the L1 and L2 stages

(A) The GFP- and mCherry-tagged alleles of *lin-28(ma426[lin-28::gfp])* and *lin-46(ma398[lin-46::mCherry])*. The *ma398ma459* allele harbors the "GTAT" deletion (*ma459*) in the 5′ UTR of *lin-46*, which is also tagged with mCherry at the C terminus (*ma398*).

(B) Differential interference contrast (DIC) and fluorescent images showing LIN-28 and LIN-46 expression in wild-type L2- (first row) and L4 (last row)-stage larvae and in *lin-28(lf)* and *lin-46(ma398ma459)* L2-stage larvae. Scale bar: 10 μm.

(C) Summary of the LIN-28 and LIN-46 expressions observed during larval stages of wild-type, *lin-28(lf)*, and *lin-46(gf/ma398ma459)* animals.

See also Figures S1 and S2 and Tables S1 and S2.

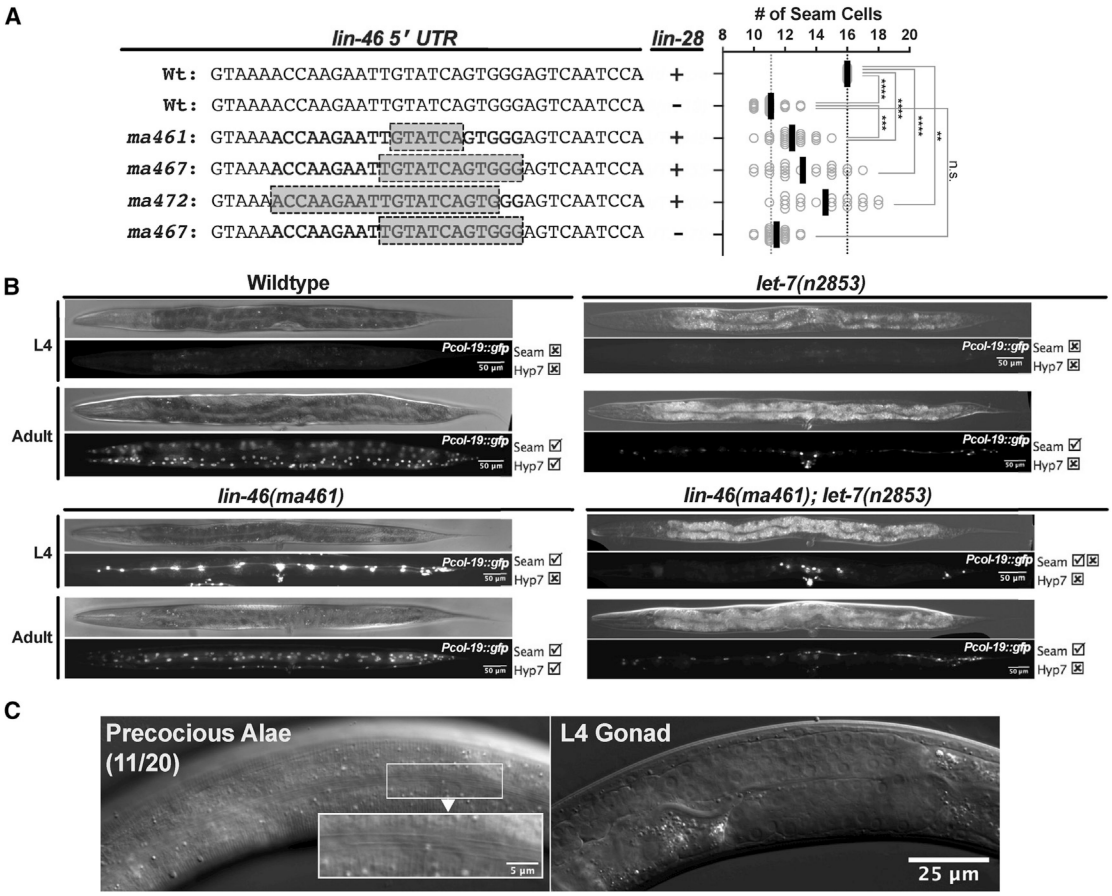

Figure 2. Precocious LIN-46 expression causes precocious cell-fate transitions in hypodermal seam cell lineage

(A) Number of seam cells observed in young adults (n = 20) of wild-type, *lin-28(lf)*, three *lin-46(gf)* mutants (*ma461*, *ma467*, and *ma472*), and *lin-28(lf); lin-46(ma467gf)* double mutants. The Student's t test was used to calculate statistical significance: Not significant (n.s.) $p > 0.05$; **$p < 0.01$; ***$p < 0.001$; and ****$p < 0.0001$. The vertical bars show the average seam cell numbers observed in 20 animals.

(B) Representative (n = 20) DIC and fluorescent images (*col-19p::gfp (maIs105)*) of L4- and adult-stage animals. Scale bar: 50 µm.

(C) DIC images of a *lin-46(ma461gf)* larva showing the (precocious) adult-specific cuticle structure called alae (precocious alae in 55% of n = 20) on the cuticle of a larva at the L4 stage indicted by the developmental stage of the gonad. Scale bar: 25 µm and 5 µm (inset). See also Table S2.

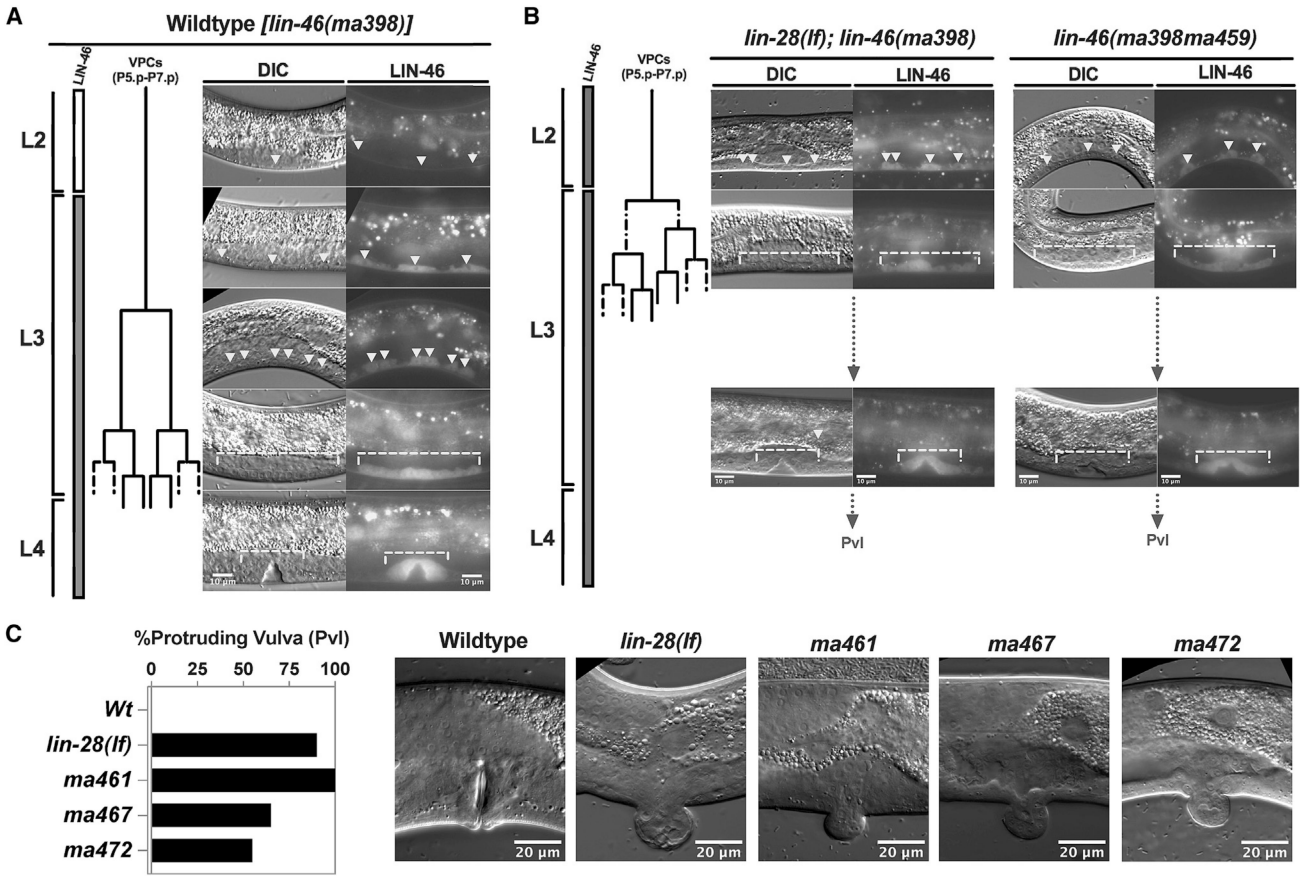

Figure 3. LIN-46 is expressed in the vulval precursor cells (VPCs), and precocious LIN-46 expression leads to precocious onset of vulva development

(A) The cell lineage diagram of the VPCs, and DIC and fluorescent images showing LIN-46::mCherry expression (from *lin-46(ma398[lin-46::mCherry])*) in the VCPs and their progeny (indicated by arrowheads or brackets). Scale bar: 10 µm.

(B) Precocious vulva development and LIN-46 expression (100%; n = 10) in *lin-28(lf)* and *lin-46(gf)* (*lin-46(ma398ma459)*). Scale bar: 10 µm.

(C) Percent protruding vulva (Pvl) phenotypes (n = 20) and DIC images showing normal vulva or Pvl morphology. Scale bar: 20 µm.

See also Table S2.

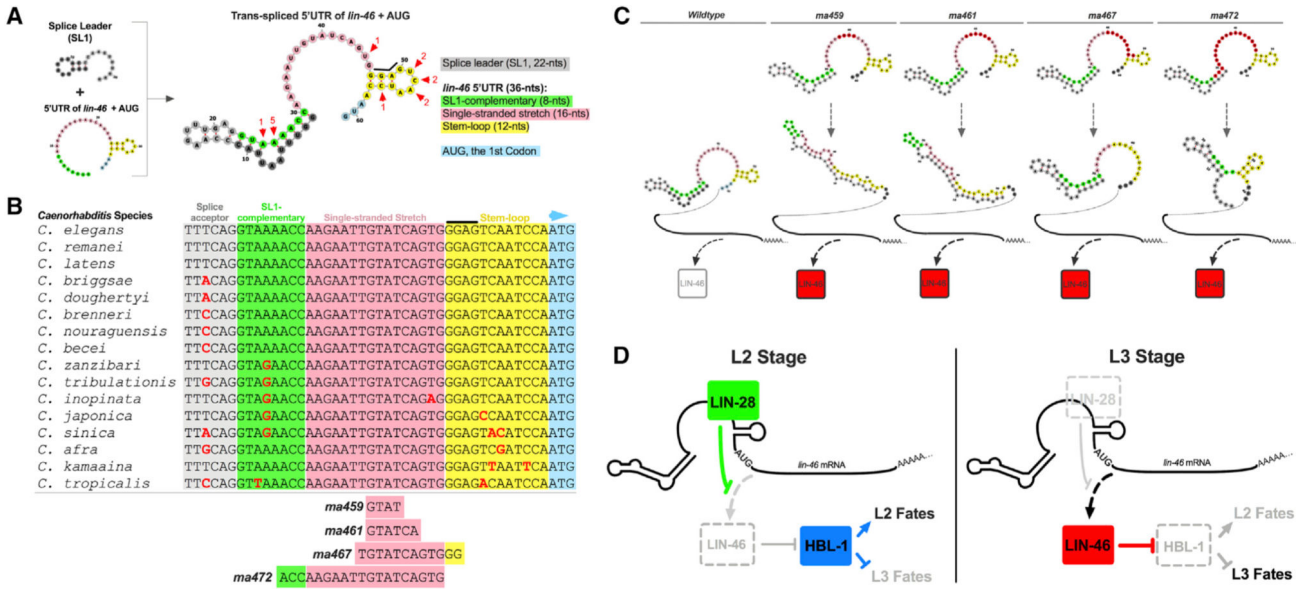

Figure 4. The conservation of the predicted architecture of the *lin-46* 5′ UTR and the effects of *lin-46(gf)* mutations on the folding of *lin-46* 5′ UTR

(A) The predicted structure of the *trans*-spliced *lin-46* 5′ UTR. Red arrowheads indicate nucleotides that are variable among the nematode species listed in (B); numbers denote the number of variations at the position indicated.

(B) An alignment of the genomic sequences encoding the *lin-46* 5′ UTR in various *Caenorhabditis* species. Nucleotides deleted in the four *lin-46(gf)* mutants examined in this study (Figures 1, 2, 3, and 4) are denoted below the alignment.

(C) Comparison of the predicted secondary structures of the *trans*-spliced *lin-46* 5′ UTR for the wild type and four *lin-46(gf)* mutants, along with schematic representation of high (red) versus low or no (clear) LIN-46 expression at the L2 stage determined by examining the expression levels of endogenously tagged *lin-46* (Figure 1) or inferred from the seam cell phenotypes (Figure 2A). For each mutation, the deleted nucleotides are highlighted in red in the wild-type structure.

(D) Model: LIN-28 controls temporal cell fate progression by regulating LIN-46 expression via the 5′ UTR of *lin-46* mRNA. At the L2 stages, the *lin-46* mRNA is transcribed but translationally repressed due to LIN-28-mediated inhibition of translation, permitting HBL-1 to function; thus, HBL-1 promotes L2 cell fates and prevents L3 cell fates. At the L2 to L3 molt, LIN-28 expression is diminished, and this allows accumulation of LIN-46, which opposes HBL-1 activity, thus preventing expression of L2 cell fates at the L3 stage.

KEY RESOURCES TABLE

REAGENT or RESOURCE	SOURCE	IDENTIFIER
Bacterial and virus strains		
E.Coli: HB101	Caenorhabditis Genetics Center (CGC)	N/A
Critical commercial assays		
SuperScript IV	Invitrogen	Cat# 18091050
FastSYBR Mixture	CoWin Biosciences	Cat# CW2621M
T7 RNA polymerase	New England Biolabs, Inc	Cat# M0251S
Experimental models: Organisms/strains		
C. elegans: strain VT3737: *lin-28(ma426[lin-28::gfp] I; lin-46(ma398[lin-46::mCherry] V*	This paper	VT3737
C. elegans: strain VT3652: *lin-28(n719) I; lin-46(ma398[lin-46::mCherry] V*	This paper	VT3652
C. elegans: strain VT3847: *lin-28(ma426[lin-28::gfp] I; lin-46(ma398ma459[DGTAT::lin-46::mCherry] V*	This paper	VT3847
C. elegans: strain VT1367: *maIs105 (Pcol-19::gfp) V*	Ambros Laboratory	VT1367
C. elegans: strain VT790: *lin-28(n719) I; maIs105 V*	Ambros Laboratory	VT790
C. elegans: strain VT3849: *lin-46(ma461) maIs105 V*	This paper	VT3849
C. elegans: strain VT3855: *lin-46(ma467) maIs105 V*	This paper	VT3855
C. elegans: strain VT3860: *lin-46(ma472) maIs105 V*	This paper	VT3860
C. elegans: strain VT3979: *lin-28(n719) I; lin-46(ma467) maIs105 V*	This paper	VT3979
C. elegans: strain VT3980: *lin-46(ma461) maIs105 V; let-7(n2853) X*	This paper	VT3980
Software and algorithms		
GraphPad Prism 8	GraphPad Software Inc. (https://www.graphpad.com/scientific-software/prism/)	RRID:SCR_002798
ZEN (blue edition)	Carl Zeiss Microscopy. (https://www.zeiss.com/microscopy/us/products/microscope-software/zen.html)	RRID:SCR_013672
ImageJ - Fiji	Open Source: (https://fiji.sc/)	RRID:SCR_002285